

Jarosław GAWRYLUK ¹

Stability of the thin-walled angle column made of bio-laminate versus glass-laminate under axial compression – numerical study

Received 17 July 2022, Revised 25 January 2023, Accepted 27 January 2023, Published online 10 February 2023

Keywords: bio-laminates, buckling, thin-walled structures, FEM, eigenproblem

The aim of this study was to determine how the change of glass laminate fibres to flax fibres will affect the stability of thin-walled angle columns. Numerical analyses were conducted by the finite element method. Short L-shaped columns with different configurations of reinforcing fibres and geometric parameters were tested. The axially compressed structures were simply supported on both ends. The lowest two bifurcation loads and their corresponding eigenmodes were determined. Several configurations of unidirectional fibre arrangement were tested. Moreover, the influence of a flange width change by $\pm 100\%$ and a column length change by $\pm 33\%$ on the bifurcation load of the compressed structure was determined. It was found that glass laminate could be successfully replaced with a bio-laminate with flax fibres. Similar results were obtained for both materials. For the same configuration of fibre arrangement, the flax laminate showed a lower sensitivity to the change in flange width than the glass material. However, the flax laminate column showed a greater sensitivity to changes in length than the glass laminate one. In a follow-up study, selected configurations will be tested experimentally.

1. Introduction

Fibrous laminates are a very popular construction material that is widely used in a growing number of industries. This is due to high strength, low weight and reduced production costs of these materials. The production of synthetic fibre-reinforced composites entails high energy demand and many limitations regarding their recycling [1, 2]. An important aspect of environment protection is to promote

✉ Jarosław Gawryluk, e-mail: j.gawryluk@pollub.pl

¹Department of Applied Mechanics, Faculty of Mechanical Engineering, Lublin University of Technology, Lublin, Poland. ORCID: 0000-0001-5075-5207



© 2023. The Author(s). This is an open-access article distributed under the terms of the Creative Commons Attribution (CC-BY 4.0, <https://creativecommons.org/licenses/by/4.0/>), which permits use, distribution, and reproduction in any medium, provided that the author and source are cited.

ecological structures made of bio-laminates with natural fibres or natural matrix. For structural applications, plant-derived fibres such as coconut, flax, jute, hemp, sisal and bamboo have desired mechanical properties and at the same time they are more economic and environment-friendly than even fiberglass [3, 4]. In terms of environmental protection, natural fibres are easier to recycle and dispose of compared to synthetic fibres. Bio-laminates reinforced with natural fibres are applied in various industries. Natural flax fibres are used in the production of door panels, window posts or car trunk inserts, musical instruments, kayaks, hockey sticks, and snowboards [5–8].

Epoxy laminates reinforced with flax fibres are more and more often investigated. Among others, there are studies describing the properties of flax fibres [9–11], relationships between the manufacturing process and the mechanical properties of laminates with flax fibres [12], and mechanical properties of laminates under different loads: tension [13–15], compression [13, 16] or bending [17]. Studies on the structures made of natural composites are particularly interesting. In [18], the authors investigated the behaviour of a flax/epoxy beam laminate under compression. Three different orientations of a bidirectional tape were studied experimentally. In addition, the critical load of the analysed structure was determined analytically. The stability of a woven flax/epoxy laminate plate was considered in [19]. Experimental and numerical analyses were performed to determine the critical load of the structure. The effects of tape orientation, plate thickness and width on the compression behaviour of the plate were investigated.

The literature review showed a lack of experimental and numerical studies on the stability and failure of natural fibre composite structures. Therefore, in this study, material data of an epoxy laminate with unidirectional fibres [16] were used, and a numerical analysis of the stability of a thin-walled column under axial compression was performed. A numerical model of the axially compressed structure with different fibre arrangement configurations was designed in a similar manner as in [20–22]. The eigenproblem was solved by the finite element method using the Abaqus software. The obtained results were then compared with those obtained for a glass-laminate structure in order to determine a relationship between bifurcation loads and flange width and column length. Similar results were obtained for natural and synthetic materials. This study is the first stage of more extensive research on the post-buckling behaviour of structures and its follow-up will involve conducting experiments on real elements.

2. Validation of the FEM model of a bio-laminate structure

The first stage of the study involved verifying the FEM model of a bio-laminate structure. In [19], a rectangular plate with the dimensions of 200 mm (length), 40 mm (width) and 1.5 mm (thickness), made of woven flax/bio epoxy (WFBE) was studied. Different fibre configurations of the plate were tested. Among others, a relationship between tape orientation in two different directions (90° ; 45°) and

bifurcation loads was investigated experimentally and numerically using the Ansys software. In each analysed case, the plate consisted of two plies whose material constants were determined experimentally (Table 1). In the experiment, the workpiece was clamped on both sides over a length of 50 mm, therefore the central section of the workpiece had a reduced buckling length of 100 mm.

Table 1. Experimental material data of WFBE [19]

Elastic constants	
E_1	5.968 (GPa)
E_2	5.392 (GPa)
ν_{12}	0.396
G_{12}	1.53 (GPa)

To verify the employed modelling method, a model of the above plate was designed in the Abaqus software. The model was assigned the same boundary conditions as in [19]. Shell elements (S8R) were used to build the plate consisting of 1000 finite elements. The number of plies was determined by the layup-ply technique [23]. The S8R elements had 6 degrees of freedom in each node. Each laminate ply was described by the material data listed in Table 1. The plate was mounted between two non-deformable plates: one of them was fixed, while the other could move to simulate axial compression. The boundary conditions were imposed on the ends of the plate in order to simulate a clamped-clamped plate. The rigid plates were modelled with R3D4 discrete rigid elements, each element having 6 degrees of freedom in each node. As a result of numerical modelling, bifurcation loads and corresponding buckling modes were determined. The first lowest buckling mode with one half-wave along the entire length of the plate was analysed (Fig. 1).

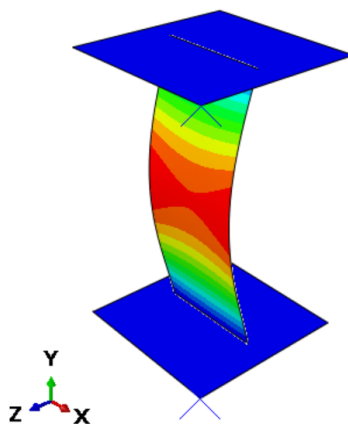


Fig. 1. First buckling mode of the tested plate

The FEM results were then compared with the experimental results reported in [19], as shown in Table 2. The FEM results and the experimental findings in [19] show high agreement, with the relative error (Error = $((PEXP - PFEM)/PEXP) * 100\%$) being below 3%. This confirms that bio-laminates were correctly modelled in Abaqus.

Table 2. Bifurcation load of a clamped-clamped plate

Orientation	Bifurcation load in N			Error (%)
	EXP [19]	Ansys [19]	FEM	
90	80.32	85.88	81.68	-1.69
45	67.89	68.71	66.48	2.07

3. Numerical model

In the next step, thin-walled angle columns made of a unidirectional flax prepreg under axial compression were investigated. Five fibre arrangement configurations with five different lengths and five different flange widths were tested. The tested cases are given in Table 3.

Table 3. Analysed cases of thin-walled columns

Lay-up configuration		Length (mm)		Width (mm)	
C1	[0/60/60/0]s	L1	200	W1	20
C2	[60/0/60/0]s	L2	250	W2	30
C3	[0/-60/60/0]s	L3	300	W3	40
C4	[-60/0/60/0]s	L4	350	W4	50
C5	[-60/60/-60/0]s	L5	400	W5	60

The tested columns were made of two materials: unidirectional flax fibre epoxy prepreg [16] and unidirectional glass fibre epoxy prepreg [24–26]. The first material's parameters were determined in the experiments reported in [16]. However, mechanical properties of the GFRP laminate were determined on the basis of tensile tests, compression tests and a shear test carried out in accordance with the relevant standards presented in papers [24–26]. These parameters are listed in Table 4. The prepreg's single ply had a thickness of 0.25 mm.

Table 4. Parameters of the tested materials

Elastic constants		
	Flax [16]	Glass [24]
E_{11} (GPa)	32	38.5
E_{22} (GPa)	5.23	8.1
ν_{12} (-)	0.396	0.270
G_{12} (GPa)	1.66	2.0

A numerical model of a compressed simply supported angle column was designed in the Abaqus software by the finite element method (Fig. 2). The laminated column was modelled using S8R shell elements having 6 degrees of freedom in each node. A regular mesh with an element size of 2 mm was used, which resulted in a total of 6000 finite elements (L3W3). Assuming that a single ply had a thickness of 0.25 mm [16], five configurations were obtained for analysis, each comprising 8 plies (Table 3). Consequently, the tested structure had a thickness of 2 mm. The lay-up of laminate plies was prepared by the layup-ply technique [23]. The tested column was simply supported on both ends, so it was put between two non-deformable plates that were modelled using discrete rigid elements R3D4 with 6 degrees of freedom in each node. At the column/plate contact, the degrees of freedom perpendicular to the column surface were constrained. In addition, contact interactions were applied between these elements. The top rigid plate was fixed to the reference point RP1 with zero degrees of freedom (motionless point). The bottom plate was fixed to the reference point RP2 and was allowed movement along the axis of the column (Z axis). Axial compression on the column was induced by the bottom cross-beam movement in the Z-axis direction. For each analysed variant, identical boundary conditions were applied.

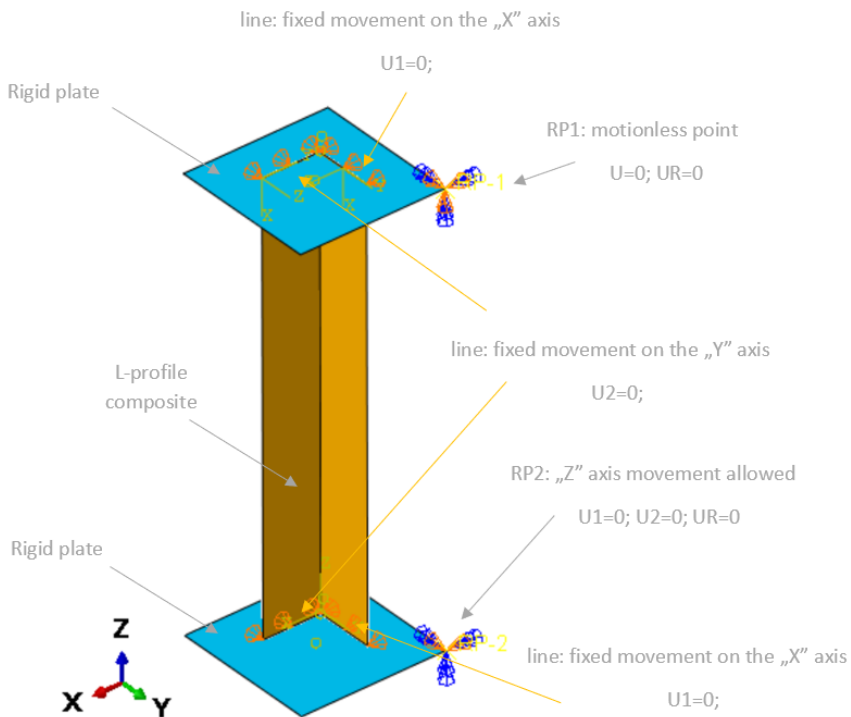


Fig. 2. Boundary conditions of the numerical model

In the numerical simulations, an eigenvalue problem was solved using the minimum potential energy criterion. A focus was put on analysing the lowest eigenmode, and the effect of prepreg fibre arrangement configurations on the eigenvalue was determined. The numerical tests were an introduction to conducting experiments on selected configurations of bio-laminate fibres. The experiments will be conducted in the next stage of the research.

4. Numerical results

The first and second eigenmodes and the corresponding bifurcation loads for all configurations of laminate plies were determined. For all cases, the lowest local buckling mode assumed the form of a half-wave on each web of the angle section (Fig. 3a). This behaviour resulted from the stress concentration in the corner of the angle section, hence the free edge of the wall would undergo the simplest buckling deformation into one half-wave. The end sections of the structure remained stationary. The second mode in each variant was characterized by the occurrence of two half-waves on each side of the column (Fig. 3b). All values of the bifurcation forces for a length of 300 mm and different widths (W1–W5) are summarized in Table 5.

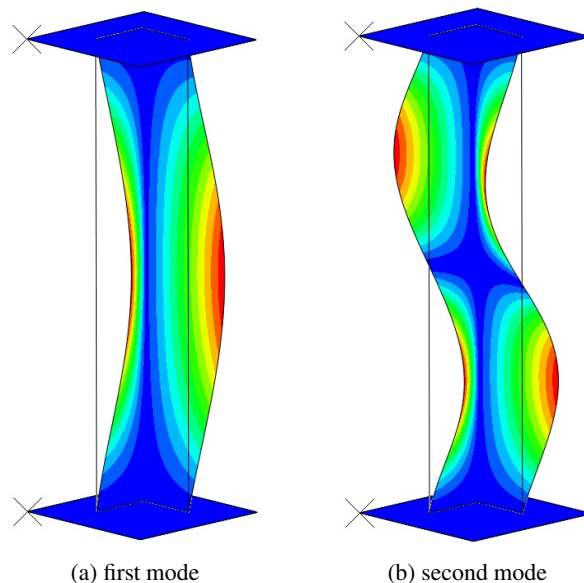


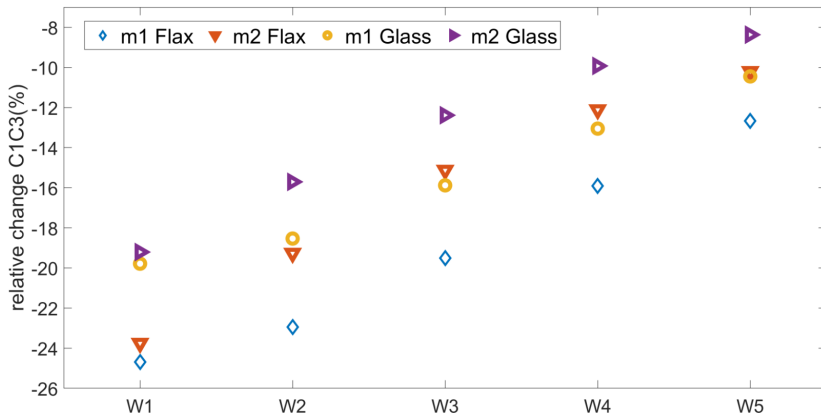
Fig. 3. Eigenmodes of the analysed bio-laminate angle column (fibre configuration has no impact)

The obtained results were analysed in terms of determining the effect of fibre arrangement configuration on each tested width variant. Both materials showed similar dependencies, which means that bifurcation load decreased with increase in

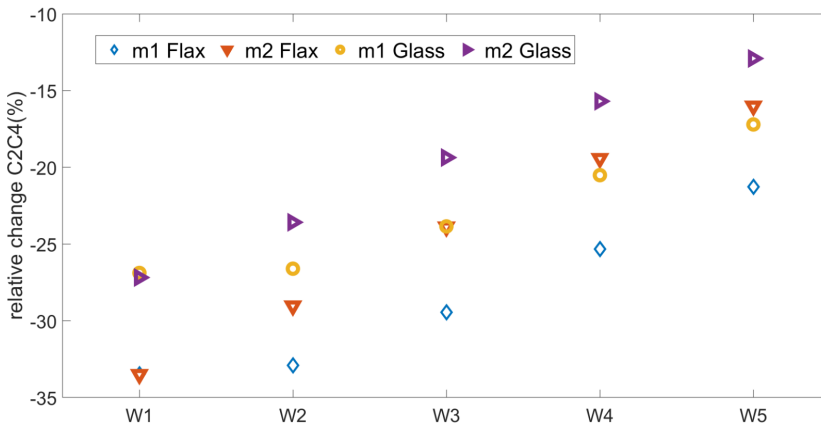
Table 5. Bifurcation loads in N for a thin-walled column (constant length)

Flax, L = 300 mm		W1	W2	W3	W4	W5
C1	mode1	1802.5	1499	1350.4	1287.4	1272.9
	mode2	2151	1929.8	1889.3	1926.5	1998.3
C2	mode1	1930	1577.8	1394.4	1305.7	1270.6
	mode2	2182.7	1878.9	1776	1764.8	1796.4
C3	mode1	2247.6	1842.9	1613.8	1492.3	1434.2
	mode2	2662	2301.6	2175.1	2159.8	2202.2
C4	mode1	2576.3	2097.1	1805	1636.4	1540.9
	mode2	2913.9	2424.4	2200.2	2107.6	2084
C5	mode1	3369	2836.9	2379.1	2065.3	1850.5
	mode2	3862.4	3085.7	2605.4	2315.6	2135.3
Glass, L = 300 mm		W1	W2	W3	W4	W5
C1	mode1	2326.2	1925.5	1720.3	1625.8	1594.5
	mode2	2762.9	2451.1	2374.7	2402	2477.1
C2	mode1	2569.6	2099.3	1843.9	1713.2	1653.3
	mode2	2904.5	2482.2	2323.8	2287.3	2308.7
C3	mode1	2786.5	2282.4	1993.5	1838	1761.1
	mode2	3293.6	2836.1	2668.8	2640.4	2684.4
C4	mode1	3260.4	2657.9	2283.7	2064.6	1937.8
	mode2	3694	3067.6	2773.8	2646.3	2606.7
C5	mode1	4214.6	3550.7	2981.2	2590.9	2323.8
	mode2	4838	3875.9	3280.2	2921.8	2699.4

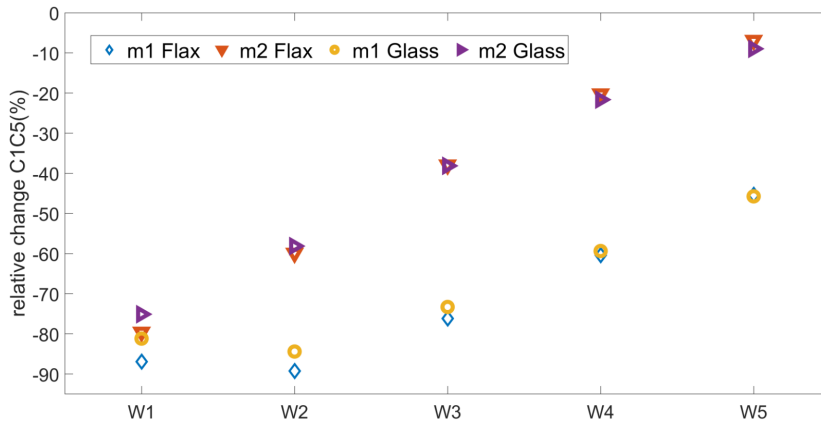
width. For the smallest width (W1) and similar configurations C1 and C3 (Fig. 4a), the relative error for the first mode was equal to 25%. When the flange width was increased, this error would decrease until it reached about 13% for the W5 width. The same situation was observed for the second mode. However, the laminate with natural fibres showed a greater sensitivity to the change in the C1/C3 configuration. As a result of changing the angle of the fibres in one ply from $+60^\circ$ to -60° , the C3 configuration showed higher stiffness than the C1 configuration. Equally similar results were obtained for the configurations C2 and C4 (Fig. 4b), i.e., the C4 system was characterized by 33% higher stiffness than C2 for width W1. On the other hand, as the flange width increased, the difference in stiffness decreased to approx. 21%. Similar results were obtained for the first and the second mode. A comparison of the C1 and C5 configurations (Fig. 4c) demonstrated that for the W1 system the first mode had a higher bifurcation load by 87%. The same trend was observed for the first mode, and with a flange width increase the difference was reduced to 45%. Regarding the second mode, a slightly different phenomenon was observed, i.e., there was a linear change between W1 and W5, with the difference in relative error



(a)



(b)



(c)

Fig. 4. Bifurcation load versus flange width change: (a) C1/C3, (b) C2/C4, (c) C1/C5

between W1 and W5 being 72% and 65% for the natural and synthetic material, respectively. Therefore, for the second mode, the flange width had a significant effect on the bifurcation load. All above cases are presented in Fig. 4, where the relative changes were calculated as follows: $\text{relative_change_C1C3} = ((F_{c1} - F_{c3})/F_{c1}) * 100\%$; $\text{relative_change_C2C4} = ((F_{c2} - F_{c4})/F_{c2}) * 100\%$; $\text{relative_change_C1C5} = ((F_{c1} - F_{c5})/F_{c1}) * 100\%$.

After that, the effect of the flange width change by $\pm 100\%$ on the bifurcation load was determined. This was done by calculating the relative change of obtained load values for W1 and W5 in relation to W3. A similar trend was observed for both materials, i.e., a reduction in the flange width by 100% resulted in a significant increase (even up to 45%) in the bifurcation load (for the first and second modes). However, an increase in the flange width by 100% did not yield similar results. A reduction in the strength of max. 23% was observed for the first mode. For the second mode, the configurations C1, C2, C3 of the natural material achieved slightly higher loads than with a smaller column width. The glass laminate behaved similarly for the C1, C3 configurations. Moreover, the natural material showed a lower sensitivity to the change in the flange width for the same configurations of fibre arrangement. This situation was observed for all tested configurations, except for C5 where no difference was observed between the results of both materials. Detailed results of the analyses are given in Fig. 5, where the relative change W3/W1 was calculated from the formula: $\text{relative_change} = ((F_{W3} - F_{W1})/F_{W3}) * 100\%$ or $((F_{W3} - F_{W5})/F_{W3}) * 100\%$.

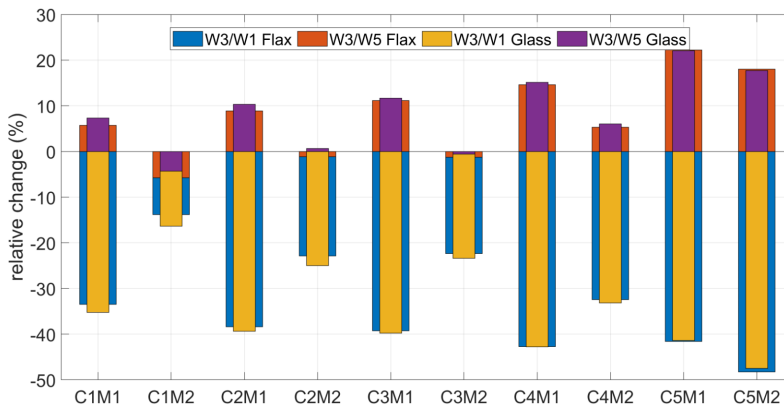


Fig. 5. Change in W3 configuration bifurcation load as a function of flange width change by $\pm 100\%$, where M1 denotes mode 1, M2 denotes mode 2

An analysis of the first two eigenmodes revealed that with a column width increase, the second mode was farther from the first one. This situation was observed for all configurations except C5 where the flange width change had no effect on the proximity between the two eigenvalues. Moreover, for the C5 configuration, the second eigenvalue was the closest to the first one and amounted to about 12% on

average. This was the case with two materials: flax and glass laminates. Regarding the remaining configurations, however, the flax fibre laminate had a positive effect, and its use led to a greater difference in the bifurcation loads between the first two modes. Detailed values of the relative change between mode1 and mode2 are shown in Fig. 6, where the aforementioned change was calculated in the following way: relative change M1M2 = $((F_M2 - F_M1)/F_M1) * 100\%$.

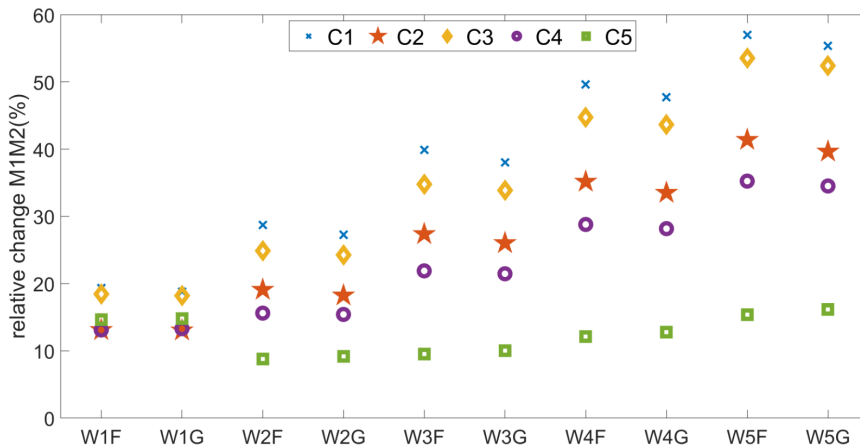


Fig. 6. Proximity between the first two eigenvalues, where F – flax, G – glass

In a successive analysis, the effect of column length on bifurcation load was investigated for both materials. Thorough tests were carried out with a constant column flange width value selected from the middle of the tested range (i.e., $W3 = 40$ mm). The obtained results are given in Table 6. As previously, the effect of fibre configuration on bifurcation load versus column length change was determined first. For this purpose, the similar configurations C1 and C3 as well as C2 and C4 were compared. Moreover, the configurations C5 and C1 were compared. A relative change was determined for every configuration pair, as shown in Fig. 7. It was found that an increase in the column length led to an increase in the relative change value for all lengths, both tested materials and each configuration pair. This showed that fibre configuration was of significant importance. It was again observed that when the column length was changed, the flax laminate was more sensitive to the change in the system configuration than the glass laminate. Furthermore, a comparison of the C5/C1 configuration pair demonstrated that the material had no impact on the relative change (Fig. 7c). On the other hand, for the C1/C3 pair, the change in the angle from 60° to -60° led to stiffening of the system. Regarding the first mode, for the L1 length, an approx. 2% increase in the stiffness of the flax laminate was obtained. As for the longest column, the natural material contributed to an over 5% increase in the column stiffness (Fig. 7a). A similar trend was observed for the second eigenmode albeit with a slightly smaller increase in stiffness. For the C2/C4 configuration pair a similar effect was obtained as for the C1/C3 pair.

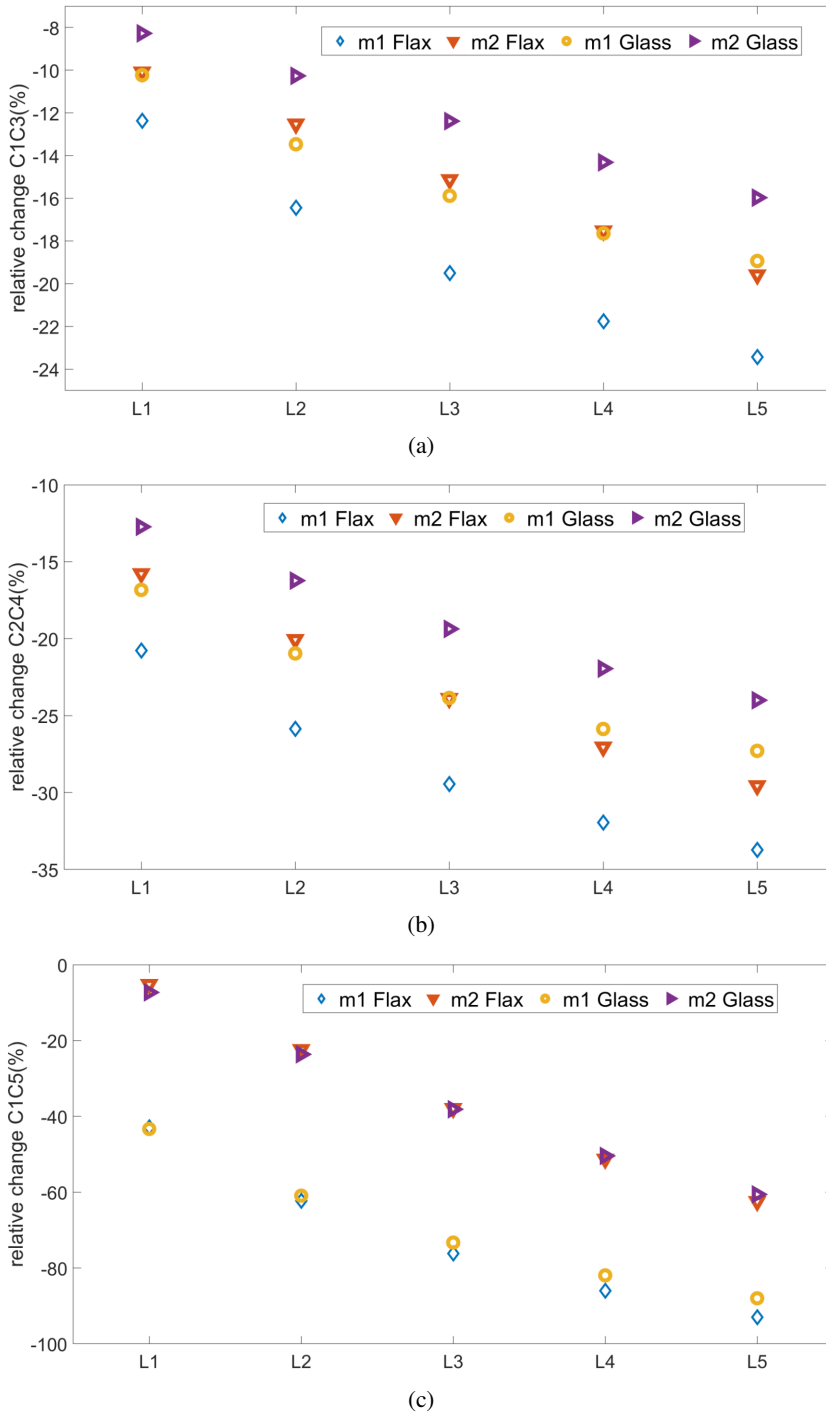


Fig. 7. Bifurcation load versus column length change: (a) C1/C3, (b) C2/C4, (c) C1/C5

Table 6. Bifurcation loads in N for a thin-walled column (constant width)

Flax, W = 40 mm		L1	L2	L3	L4	L5
C1	mode1	1833.3	1521.6	1350.4	1246.1	1177.5
	mode2	2900.7	2261.9	1889.3	1654.4	1497.4
C2	mode1	1819.1	1545.4	1394.4	1302.1	1241.1
	mode2	2589.7	2075	1776	1588.8	1464.5
C3	mode1	2060.1	1771.7	1613.8	1517.2	1453.4
	mode2	3193.3	2545.1	2175.1	1944.4	1790.7
C4	mode1	2196.9	1945.1	1805	1718.1	1659.8
	mode2	2998.2	2491.2	2200.2	2018.5	1897.4
C5	mode1	2619.9	2469.1	2379.1	2318.1	2272.7
	mode2	3050.9	2767.7	2605.4	2502.7	2432.6
Glass, W = 40 mm		L1	L2	L3	L4	L5
C1	mode1	2294.1	1923.9	1720.3	1596	1514.1
	mode2	3594.3	2823.3	2374.7	2092.3	1903.6
C2	mode1	2363.4	2029.3	1843.9	1729.9	1654.3
	mode2	3325.5	2692.8	2323.8	2091.9	1937.4
C3	mode1	2528.8	2183	1993.5	1877.6	1800.8
	mode2	3891.7	3113.1	2668.8	2391.8	2207.6
C4	mode1	2761.1	2454.6	2283.7	2177.4	2105.8
	mode2	3748.7	3129.7	2773.8	2551	2402.4
C5	mode1	3288.1	3095.8	2981.2	2903.8	2846.4
	mode2	3856.3	3490.3	3280.2	3147.5	3056.8

After that, an analysis was carried out to determine the percentage of bifurcation load change with changing the column length by ± 100 mm. The reference was a 300 mm long column (L3). The analysis was performed for two materials where the greatest changes in stiffness for all configurations were obtained for the second eigenmode. For almost every tested variant, the flax laminate showed a greater sensitivity to the changes in column length. Only the C5 configuration showed a slightly different result. A reduction in the sample length by 100 mm caused a greater change in the bifurcation load than increasing the length to 400 mm. The highest increase in column stiffness for the first mode was observed for the C1 configuration (it increased by about 35%). A reduction in the sample length for the same C1 configuration was found to have the greatest effect on the load value (approx. 13%). For the second eigenmode, the stiffness change was -55% and 21%, respectively. The relative change value for L3/L1 and L3/L5 was calculated from the formula: $\text{relative change} = ((F_{L3} - F_{L1})/F_{L3}) * 100\%$ or $((F_{L3} - F_{L5})/F_{L3}) * 100\%$. All results are presented in Fig. 8.

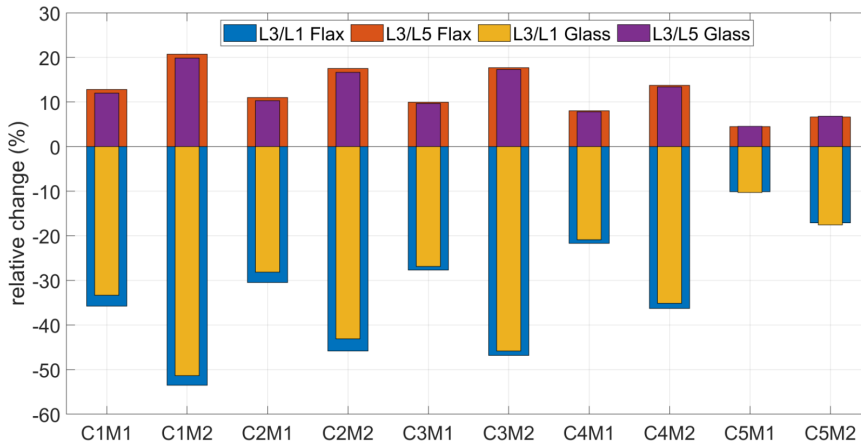


Fig. 8. Percentage bifurcation load change for the shortest (L1) and longest (L5) column in relation to a length of 300 mm (L3), where M1 – mode 1, M2 – mode 2

Above it was described how the change in column length affected the proximity between the first two modes (Fig. 9). Totally different results were obtained for width change. Namely, with an increase in column length, the first two eigenvalues become closer and closer to each other (C1–C4). In addition, it was found that for the same configurations (C1–C4), the natural laminate caused slightly greater differences in the first two eigenvalues. However, for the C5 configuration, the column length change did not significantly affect the proximity between mode 1 and mode 2, even though the natural laminate exhibited a lower sensitivity to column length change than the glass laminate.

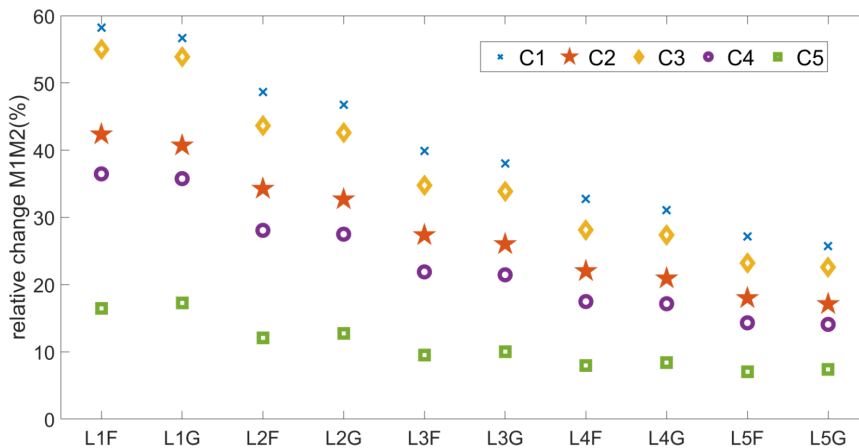


Fig. 9. Proximity between the first two eigenvalues for a constant value of flange width; F – flax laminate, G – glass laminate

In the next step of this study, the post-buckling behaviour of the angle columns was investigated. A nonlinear buckling problem was solved by the Newton-Raphson method using FEM-based commercial software. The amplitude of initial geometrical imperfection related to the lowest local buckling mode was set to 0.01 mm. The numerical model and its boundary conditions were the same as in the eigenvalue problem. The post-buckling behaviour of the selected column is illustrated via load versus shortening plots (i.e., $P - \Delta$ plots in Figs. 10, 11), where the solutions achieved for the flax prepreg and the glass prepreg are compared. Due to a large number of calculation variants, only selected cases were analysed in detail. First, a column made of flax and glass prepreg with the greatest length was selected (i.e., Sample L5 with a length of 400 mm and configuration C5 – Fig. 10). By the same token, simulations were carried out for the shortest column (i.e., Sample L1 with a length of 200 mm and configuration C5 – Fig. 10). The shortest and the longest angles made of flax and glass prepreps were tested. As expected, the longer sample showed a greater shortening than the shorter one. Moreover, the glass prepreg specimens showed a greater stiffness in the pre-buckling and post-buckling states than the specimens having identical length that were made of the natural material. In the nonlinear analysis, the longer samples (L5) loaded with a force of 7000 N exhibited 35% more shortening than the shorter samples (L1). It is worth noting that this relationship was observed for both analysed materials. The pre-buckling and post-buckling states in Fig. 10 are marked with straight lines. Moreover, for all obtained curves it is possible to observe a break point, i.e., the point which marks the critical state [27, 28].

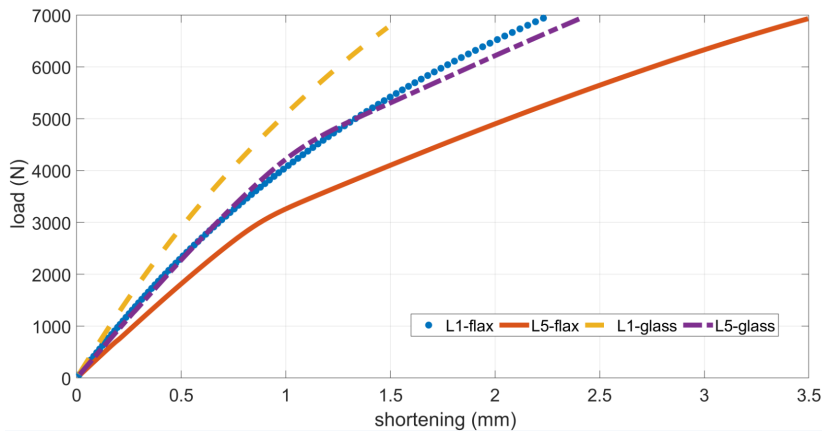


Fig. 10. Post-buckling behaviour of the analysed columns with a ply arrangement of $[-60/60/-60/0]_s$ (C5) and constant width of 40 mm (W3) when the amplitude of initial deflection is equal to 0.01 mm

Additionally, the analysis covered the columns with C1 configuration and a constant length of 300 mm (i.e., L3) and a variable flange width. Fig. 11 shows the $P - \Delta$ plot for the smallest and the largest flange width. The behaviour of the

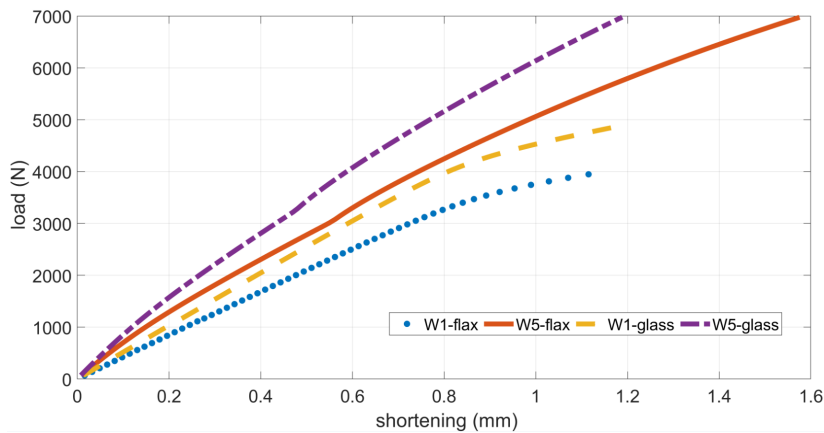


Fig. 11. Post-buckling behaviour of the analysed columns with a ply arrangement of $[0/60/60/0]_s$ (C1) and constant length of 300mm (L3) when the amplitude of initial deflection is equal to 0.01 mm

columns made of flax laminate and glass fibre laminate was analysed in detail. With wider flanges (i.e., 60 mm, W5), the columns showed a greater stiffness in the pre-buckling and the post-buckling condition. This observation was made for the column made of both natural and synthetic laminate. Moreover, for the 60mm width sample (i.e., W5) with a shortening of about 1.2 mm, the compressive load was higher by approx. 44% and 40% for the synthetic and the natural material, respectively, than that obtained for the column with a flange width of 20 mm (i.e., W1). However, for the flax sample (W5) loaded with the same compressive force of 7000N, the shortening was greater by about 32% compared to the glass sample (W5). The numerical calculations for W1 were prematurely terminated due to no convergence of the solution.

5. Conclusions

The stability of a thin-walled laminate angle under axial compression was analysed numerically. Numerical simulations were performed by the finite element method using the Abaqus software. Two materials were tested: unidirectional flax fibre epoxy prepreg and unidirectional glass fibre epoxy prepreg. The first and second local eigenmodes of the structure were analysed. Five different configurations of unidirectional prepreg fibres were tested. The influence of flange width and column length on the stability of the system was determined. A column with a flange width ranging from 20 mm to 60 mm was tested. The length of the column under study ranged from 200 mm to 400 mm.

Detailed numerical analyses showed that the short flax laminate angles under compression were sensitive to the angle of reinforcing fibre arrangement. It was found that the lowest bifurcation load value decreased with an increase in the flange

width for all tested cases. A similar behaviour was observed for the second eigenmode with a small column width, while starting with 40mm the effect of width change was less and less significant. A similar phenomenon was also observed for the glass fibre laminate. Reducing the flange width by 100% (for both materials) resulted in a significant increase (up to 45%) in the bifurcation load (for the first and second modes). However, increasing the flange width by 100% did not have an opposite effect (max to -20%). The flax laminate showed a lower sensitivity to the flange width change for the same configuration of fibre arrangement. This observation was made for all tested configurations, except for C5 where no difference was observed between the results of both materials.

After that, it was determined how the bifurcation loads depended on the column length (in the range of 200–400 mm) when the flange width value was maintained constant. The greatest changes in the bifurcation loads for all configurations were obtained for the second eigenmode (up to 54% for L1). In the almost every tested variant, the flax laminate showed a greater sensitivity to the column length change than the glass laminate. The C5 configuration was the only one with a slightly different result. Nevertheless, a decrease in the sample length by 100 mm generally caused a greater change in the bifurcation load than increasing the column length to 400 mm.

A comparison of the similar C1 and C3 configurations revealed that for a column length of 300 mm, a reduction in the flange width resulted in a smaller discrepancy between the results (for both modes and materials). As a result of changing the angle of the fibres in one ply from +60° to -60°, the C3 configuration exhibited a higher stiffness than the C1 configuration. However, the flax laminate showed a greater sensitivity to the change in the C1/C3 configuration. Similar results were obtained as for the C2 and C4 configurations. For the C5/C1 configurations (with $L = 300$ mm), an increase in the stiffness of up to 87% (flax) and 81% (glass) was obtained for the lowest flange width (W1M1). As the width decreased, the effect decreased. It was observed that the second eigenvalue was the most considerably affected by the column width change for those configurations. The difference in the results between W1–W5 was 72% and 65% for the flax and the glass laminate, respectively. The results of the column with a fixed width (40 mm) demonstrated that an increase in the column length resulted in reduced bifurcation loads. A comparison of the C3/C1 and C4/C2 configurations showed that the eigenvalues moved away from each other with increasing column length. Thus, the effect of the configuration type became more and more visible. Furthermore, the flax laminate was more sensitive to the change in the system configuration than the glass laminate (by 2–5%). A comparison of the C5/C1 configurations showed that the material type had hardly any effect on the relative error value obtained for those configurations. The C5 configuration showed the highest stiffness of all tested systems.

An analysis of the obtained results in terms of proximity between the first two modes demonstrated that the C5 configuration showed the lowest resistance,

as the difference in the eigenvalues ranged between 7 and 16%. Moreover, the change in the column length and width had no effect on the obtained percentage differences between the adjacent modes (M1 and M2). Regarding the remaining configurations (C1–C4), as the flange width increased, the proximity between the eigenvalues became more and more diverged (up to 55%), while an opposite effect was observed when the column length was increased. Furthermore, a slightly higher discrepancy between the neighbouring eigenvalues was observed for the natural material.

After that, the post-buckling behaviour of selected columns (made of flax and glass prepreps) was investigated. Nonlinear buckling problems were also solved using FEM. It was tested how the length of the column affects the post-buckling behaviour of the system with the same configuration and flange width (C5, W3). A similar behaviour was observed for both tested materials, i.e., the longer samples showed a greater shortening than the shorter ones. Additionally, the columns with the C1 configuration and a constant length (L3) and variable flange width were tested. The columns with wider flanges showed a greater stiffness in the post-buckling range (for both materials).

Considering the results, it can be concluded that the laminate fibre arrangement has a significant impact on the characteristics of an L-profile column. The behaviour of the column also depends on the material type. Therefore, when choosing material, it is worth considering the natural material as it shows a similar behaviour as the glass fibre material, but has a much more favourable impact on the environment. The results of this study will serve as a basis for further research in which a nonlinear range will be investigated. Further studies will also involve conducting experiments on real bio-laminate angle columns.

Acknowledgements

The research was conducted under project No. 2021/05/X/ST8/00396 financed by the National Science Centre, Poland. Special acknowledgements are due to Professor Andrzej Teter from Lublin University of Technology for scientific support and valuable discussions.

References

- [1] S.V. Joshi, L.T. Drzal, A.K. Mohanty, and S. Arora. Are natural fiber composites environmentally superior to glass fiber reinforced composites? *Composites Part A: Applied Science and Manufacturing*, 35(3):371–376, 2004. doi: [10.1016/j.compositesa.2003.09.016](https://doi.org/10.1016/j.compositesa.2003.09.016).
- [2] P. Wambua, J. Ivens and I. Verpoest. Natural fibers: can they replace glass in fiber reinforced plastics? *Composites Science and Technology*, 63(9):1259–1264, 2003. doi: [10.1016/S0266-3538\(03\)00096-4](https://doi.org/10.1016/S0266-3538(03)00096-4).
- [3] D.B. Dittenber and H.V.S. GangaRao. Critical review of recent publications on use of natural composites in infrastructure. *Composites Part A: Applied Science and Manufacturing*, 43(8):1419–1429, 2012. doi: [10.1016/j.compositesa.2011.11.019](https://doi.org/10.1016/j.compositesa.2011.11.019).

- [4] A. Stamboulis, C.A. Baillie, and T. Peijs. Effects of environmental conditions on mechanical and physical properties of flax fibers. *Composites Part A: Applied Science and Manufacturing*, 32(8):1105–1115, 2001. doi: [10.1016/S1359-835X\(01\)00032-X](https://doi.org/10.1016/S1359-835X(01)00032-X).
- [5] L. Pil, F. Bensadoun, J. Pariset, and I. Verpoest. Why are designers fascinated by flax and hemp fiber composites? *Composites Part A: Applied Science and Manufacturing*, 83:193–205, 2016. doi: [10.1016/j.compositesa.2015.11.004](https://doi.org/10.1016/j.compositesa.2015.11.004).
- [6] H.Y. Cheung, M.P. Ho, K.T. Lau, F. Cardona, and D. Hui. Natural fiber-reinforced composites for bioengineering and environmental engineering applications. *Composites Part B: Engineering*, 40(7):655–663, 2009. doi: [10.1016/j.compositesb.2009.04.014](https://doi.org/10.1016/j.compositesb.2009.04.014).
- [7] M.I. Misnon, Md M. Islam, J.A. Epaarachchi, and K.T. Lau. Potentiality of utilising natural textile materials for engineering composites applications. *Materials & Design*, 59:359–368, 2014. doi: [10.1016/j.matdes.2014.03.022](https://doi.org/10.1016/j.matdes.2014.03.022).
- [8] T. Gurunathan, S. Mohanty, and S.K. Nayak. A review of the recent developments in biocomposites based on natural fibers and their application perspectives. *Composites Part A: Applied Science and Manufacturing*, 77:1–25, 2015. doi: [10.1016/j.compositesa.2015.06.007](https://doi.org/10.1016/j.compositesa.2015.06.007).
- [9] H.L. Bos, M.J.A. Van Den Oever, and O.C.J.J. Peters. Tensile and compressive properties of flax fibers for natural fiber reinforced composites. *Journal of Materials Science*, 37:1683–1692, 2002. doi: [10.1023/A:1014925621252](https://doi.org/10.1023/A:1014925621252).
- [10] C. Baley. Analysis of the flax fibers tensile behavior and analysis of the tensile stiffness increase. *Composites Part A: Applied Science and Manufacturing*, 33(7):939–948, 2002. doi: [10.1016/S1359-835X\(02\)00040-4](https://doi.org/10.1016/S1359-835X(02)00040-4).
- [11] C. Baley, M. Gomina, J. Breard, A. Bourmaud, and P. Davies. Variability of mechanical properties of flax fibers for composite reinforcement. A review. *Industrial Crops and Products*, 145:111984, 2020. doi: [10.1016/j.indcrop.2019.111984](https://doi.org/10.1016/j.indcrop.2019.111984).
- [12] I. El Sawi, H. Bougherara, R. Zitoun, and Z. Fawaz. Influence of the manufacturing process on the mechanical properties of flax/epoxy composites. *Journal of Biobased Materials and Bioenergy*, 8(1):69–76, 2014. doi: [10.1166/jbmb.2014.1410](https://doi.org/10.1166/jbmb.2014.1410).
- [13] K. Strohrmann and M. Hajek. Bilinear approach to tensile properties of flax composites in finite element analyses. *Journal of Materials Science*, 54:1409–1421, 2019. doi: [10.1007/s10853-018-2912-1](https://doi.org/10.1007/s10853-018-2912-1).
- [14] Z. Mahboob, Y. Chemisky, F. Meraghni, and H. Bougherara. Mesoscale modelling of tensile response and damage evolution in natural fiber reinforced laminates. *Composites Part B: Engineering*, 119:168–183, 2017. doi: [10.1016/j.compositesb.2017.03.018](https://doi.org/10.1016/j.compositesb.2017.03.018).
- [15] Z. Mahboob, I. El Sawi, R. Zdera, Z. Fawaz, and H. Bougherara. Tensile and compressive damaged response in Flax fiber reinforced epoxy composites. *Composites Part A: Applied Science and Manufacturing*, 92:118–133, 2017. doi: [10.1016/j.compositesa.2016.11.007](https://doi.org/10.1016/j.compositesa.2016.11.007).
- [16] C. Nicolinco, Z. Mahboob, Y. Chemisky, F. Meraghni, D. Oguamanam, and H. Bougherara. Prediction of the compressive damage response of flax-reinforced laminates using a mesoscale framework. *Composites Part A: Applied Science and Manufacturing*, 140:106153, 2021. doi: [10.1016/j.compositesa.2020.106153](https://doi.org/10.1016/j.compositesa.2020.106153).
- [17] R.T. Durai Prabhakaran, H. Teftegaard, C.M. Markussen, and B. Madsen. Experimental and theoretical assessment of flexural properties of hybrid natural fiber composites. *Acta Mechanica*, 225:2775–2782, 2014. doi: [10.1007/s00707-014-1210-5](https://doi.org/10.1007/s00707-014-1210-5).
- [18] M. Fehri, A. Vivet, F. Dammak, M. Haddar, and C. Keller. A characterization of the damage process under buckling load in composite reinforced by flax fibers. *Journal of Composites Science*, 4(3):85, 2020. doi: [10.3390/jcs4030085](https://doi.org/10.3390/jcs4030085).
- [19] V. Gopalan, V. Suthenthiraveerappa, J.S. David, J. Subramanian, A.R. Annamalai, and C.P. Jen. Experimental and numerical analyses on the buckling characteristics of woven flax/epoxy laminated composite plate under axial compression. *Polymers*, 13(7):995, 2021. doi: [10.3390/polym13070995](https://doi.org/10.3390/polym13070995).

- [20] J. Gawryluk and A. Teter. Experimental-numerical studies on the first-ply failure analysis of real, thin-walled laminated angle columns subjected to uniform shortening. *Composite Structures*, 269:114046, 2021. doi: [10.1016/j.compstruct.2021.114046](https://doi.org/10.1016/j.compstruct.2021.114046).
- [21] J. Gawryluk. Impact of boundary conditions on the behavior of thin-walled laminated angle column under uniform shortening. *Materials*, 14(11):2732, 2021. doi: [10.3390/ma14112732](https://doi.org/10.3390/ma14112732).
- [22] J. Gawryluk. Post-buckling and limit states of a thin-walled laminated angle column under uniform shortening. *Engineering Failure Analysis*, 139:106485, 2022. doi: [10.1016/j.engfailanal.2022.106485](https://doi.org/10.1016/j.engfailanal.2022.106485).
- [23] ABAQUS 2020 HTML Documentation, DassaultSystemes.
- [24] T. Kubiak and L. Kaczmarek. Estimation of load-carrying capacity for thin-walled composite beams. *Composite Structures*, 119:749–756, 2015. doi: [10.1016/j.compstruct.2014.09.059](https://doi.org/10.1016/j.compstruct.2014.09.059).
- [25] T. Kubiak, S. Samborski, and A. Teter. Experimental investigation of failure process in compressed channel-section GFRP laminate columns assisted with the acoustic emission method. *Composite Structures*, 133:921–929, 2015. doi: [10.1016/j.compstruct.2015.08.023](https://doi.org/10.1016/j.compstruct.2015.08.023).
- [26] M. Urbaniak, A. Teter, and T. Kubiak. Influence of boundary conditions on the critical and failure load in the GFPR channel cross-section columns subjected to compression. *Composite Structures*, 134:199–208, 2015. doi: [10.1016/j.compstruct.2015.08.076](https://doi.org/10.1016/j.compstruct.2015.08.076).
- [27] A. Teter and Z. Kolakowski. On using load-axial shortening plots to determine the approximate buckling load of short, real angle columns under compression. *Composite Structures*, 212:175–183, 2019. doi: [10.1016/j.compstruct.2019.01.009](https://doi.org/10.1016/j.compstruct.2019.01.009).
- [28] A. Teter, Z. Kolakowski, and J. Jankowski. How to determine a value of the bifurcation shortening of real thin-walled laminated columns subjected to uniform compression? *Composite Structures*, 247, 12430, 2020. doi: [10.1016/j.compstruct.2020.112430](https://doi.org/10.1016/j.compstruct.2020.112430).